

Applicability of Hydrodynamics in Hadronic Phase of Heavy-Ion Collisions

Ronald Scaria,* Captain R. Singh,† and Raghunath Sahoo‡

Department of Physics, Indian Institute of Technology Indore, Simrol, Indore 453552, India

(Dated: September 17, 2024)

The hadronic phase and its dynamics in relativistic heavy-ion collisions are topics of immense discussion. The hadronic phase contains various massive hadrons with an abundance of the lightest hadron, i.e., π -mesons. In this work, we consider that pions are in the thermal equilibrium in the hadronic phase and use second-order massive viscous hydrodynamics to obtain its expansion to the boundary of the kinetic freeze-out. We achieve the kinetic freeze-out boundary with the Knudsen number (Kn) limit: $Kn > 1$. When this condition is met, hydrodynamics expansion breaks down, and the mean free path becomes sufficiently large in comparison with the system size so that the particle yields get preserved. Further, we investigate the effect of the massive fluid on the resonance particle yields, including re-scattering and regeneration, along with their natural decay width. These resonances can play an important role in determining the characteristics of the hadronic phase as they have sufficiently small lifetimes, which may be comparable to the hadronic phase lifetime. In the current study, we predict the hadronic phase lifetime, which is further used to determine the $K^*(892)^0/K$, $\phi(1020)/K$, and $\rho(770)^0/\pi$ ratios at the kinetic freeze-out. We obtain these ratios as a function of charged particle multiplicity and transverse momentum and compare our findings with experimental data. Our results qualitatively agree with the experimental data indicating the possible hydrodynamical evolution of the hadronic phase.

I. INTRODUCTION

Relativistic heavy-ion collisions provide a unique environment that encapsulates various phases of QCD matter. The formation of a hot and dense, locally thermalized deconfined phase of colorful partons known as Quark-Gluon Plasma (QGP) is expected to be formed in the very initial stages ($\tau < 1$ fm) following the collision. The emergence of a color-neutral hadronic phase ensues when the strongly interacting QGP phase dissipates, indicating a phase transition from a deconfined partonic phase to a colorless hadronic medium. Experimental data propose that the QGP phase exhibits behavior akin to those of a “perfect fluid” [1–4], characterized by an extremely low shear viscosity (η) to entropy density (s) ratio near the AdS/CFT bound of $1/4\pi$ [5]. The QGP, formed at a very high initial temperature, is presumed to evolve based on hydrodynamic models before cooling down to the chemical freeze-out temperature. At this temperature, all inelastic collisions cease, leading to the breakdown of QGP hydrodynamics. Many of these computations are carried out assuming the QGP phase to be both chemically and thermally equilibrated and composed of massless particles. The chemical freeze-out temperature closely aligns with the critical temperature (T_c) for phase transition predicted by lattice QCD (LQCD) calculations [6]. Using this framework, the lifetime of the QGP can be estimated in ultra-relativistic collisions [7, 8]. However, defining the lifetime of the hadronic phase (the duration between chemical and kinetic freeze-outs) becomes somewhat ambiguous without

a clear definition of the kinetic freeze-out temperature or boundary.

Multiple models have been used to study the hadronic phase produced in relativistic nuclear collisions. In one of the earliest studies [9], the authors describe the hadronic phase as a system that is thermally equilibrated but chemically decoupled. This phase allows momentum transfer between the constituent particles through collisions. The authors performed their calculations by assuming that the yields of resonances stay in equilibrium with those of the daughter particles formed from their decays. This assumption constitutes the concept of partial chemical equilibrium (PCE). This concept has been further used to determine the kinetic freeze-out temperature from the yields of hadrons and resonances [10]. Other concepts treat the hadronic phase using transport models like the Ultra-relativistic Quantum Molecular Dynamics (UrQMD) model [11] or the AMPT (A Multi-Phase Transport) model [12]. These are generally used as afterburners to the hydrodynamic calculations, as in Ref. [13, 14]. However, it has been observed that in such models, the intrinsic medium properties like viscosity are not well described [15, 16]. For example, the hadronic medium produced in UrQMD remembers the prior QGP evolution and its properties even after hadronization [15] and can lead to different evolutions for different initial conditions chosen. Also, in Ref. [17], it has been shown that the hadronic evolution itself has transport properties comparable with a low viscous fluid. Recent advancements in far-from-equilibrium hydrodynamics [18, 19] also imply the possibility of rapid thermalization even if the system is away from equilibrium. Therefore, employing hydrodynamics could thus be an alternate approach to describing the hadronic phase. Hydrodynamics treats the system as a

* ronaldscaria.rony@gmail.com

† captainriturajsingh@gmail.com

‡ Corresponding author: Raghunath.Sahoo@cern.ch

continuous, locally thermalized fluid, which allows for the use of macroscopic properties like temperature, pressure, and flow velocity to describe the evolution of the medium. This approach is more effective at capturing the collective flow and the evolution of thermodynamic quantities, which are essential for understanding the bulk properties of the system. Additionally, hydrodynamic models can naturally incorporate concepts like partial chemical equilibrium (PCE) and provide a framework for determining the hadronic phase lifetime. By maintaining a thermalized description throughout the evolution, the hydrodynamic description of the hadronic phase may offer a consistent depiction of the hadronic phase.

In this direction, the Knudsen number (Kn) can be used to study the possibility of thermalization and applicability of hydrodynamics in a medium. Low values of Kn ($Kn \ll 1$) indicate systems with low gradients of hydrodynamic quantities, and thus the system is close to equilibrium (high degree of thermalization) [20]. A similar conclusion is also obtained in Ref. [21], where the applicability of fluid dynamics is strictly valid for cases of $Kn \sim 1$. In our previous work [22], we explored the possibility of fluid dynamics in the hadronic medium by studying Kn . We observed a considerably small value for Kn at high temperatures within the excluded volume hadron resonance gas (EVHRG) formalism. In this article, we try to extend this work by explicitly deriving the valid equations for dissipative second-order hydrodynamics for a massive system and exploring the possibility of hydrodynamics in the hadronic phase by estimating the hadronic phase lifetime.

Short-lived resonances decay with a wide range of lifetimes, which allows them to be suitable probes for characterizing the properties of hadronic matter produced in heavy-ion collisions ([23] and references therein) and also to estimate the hadronic phase lifetime. The resonances produced at the chemical freeze-out boundary may decay before the kinetic freeze-out, and their decay products undergo hadronic re-scattering, leading to a decrease in their yield. At the same time, pseudoelastic interactions between hadrons can regenerate the resonances in the medium, which increases their yields. Various transport and statistical thermal model calculations show that re-scattering and regeneration processes significantly affect the final state resonance yields [6, 14, 24–28]. These effects make them perfect probes to study the hadronic phase lifetime, as explored in Refs. [23, 29]. In this work, we attempt to follow an alternate approach and use Kn to govern the cooling of a hadronic medium from T_c using a viscous second-order 1+1D hydrodynamic model to obtain the hadronic phase lifetime. We introduce a model for the evolution of resonance particle yields during the hadronic phase. This model is used within the ambit of hydrodynamic evolution to obtain the multiplicity and transverse momentum (p_T) dependent final yields, which are then

compared with experimental data.

This article is organized as follows. Sec. II details the equations derived for hydrodynamic calculations and the considerations that have been used to estimate the hadronic phase lifetime. Further, in Sec. III, the formalism to obtain resonance yields at freeze out within a kinetic approach is detailed. In Sec. IV, we present the results along with their discussion, and Sec. V summarizes our study.

II. EXPANDING HADRONIC PHASE

Lattice QCD (LQCD) calculations predict the existence of such a deconfinement transition from hadronic to partonic constituents for energy densities greater than 1 GeV fm^{-3} [30]. At zero baryochemical potential (μ_B), this deconfinement transition is predicted again by LQCD to be of crossover in nature [31] at the critical temperature, $T_c \simeq 155 \text{ MeV}$ [32–34]. The hadronic phase, thus produced at the end of the QGP phase as a result of confinement, further expands and cools down. A sophisticated interplay of hadronic interactions, such as elastic and inelastic scattering, resonance production, decay, etc., characterizes the expanding hadronic phase. To precisely interpret the experimental data and deduce the properties of the QGP and the nature of the QCD phase transition, a thorough understanding of this complex phase is essential. It can provide unique insights into the fundamental properties of matter under extreme conditions, emphasizing the necessity for modeling this dynamic phase. Here, we employ hydrodynamics to study the evolution of the hadronic medium and its cooling rate under various scenarios.

A. Temperature evolution of the hadronic medium

The hadronic medium produced at chemical freeze-out is still at a higher temperature and cools down with time. The temperature cooling can be studied by solving the first and second-order fluid dynamical equations [35–37] derived within the framework of causal Müller-Israel-Stewart theory of dissipative fluid dynamics [38–40]. In the 1+1D scaling solution we get [35, 37]

$$\frac{\partial \varepsilon}{\partial \tau} = -\frac{\varepsilon + P}{\tau} + \frac{\phi}{\tau} \quad (1)$$

The perfect fluid, first-order, and second-order theories are distinguished by ϕ , which defines the effect of viscous terms, as given below,

$$\phi = 0, \quad \text{perfect fluid} \quad (2)$$

$$\phi = \frac{4\eta}{3\tau}, \quad \text{first-order} \quad (3)$$

$$\frac{d\phi}{d\tau} = -\frac{\phi}{\tau_\phi} - \frac{\phi}{2} \left[\frac{1}{\tau} + \frac{1}{\beta_2} T \frac{d}{d\tau} \left(\frac{\beta_2}{T} \right) \right] + \frac{2}{3\beta_2\tau}, \quad \text{second-order} \quad (4)$$

where τ_ϕ is the relaxation time due to shear viscous component and $\beta_2 = \frac{\tau_\phi}{2\eta}$, η being shear viscosity. In second-order theory, ϕ indicates the characteristics of the system by measuring the change in η through Eq.4. The solution of Eq.1 and Eq.4 can be obtained numerically for a viscous system. The initial conditions for ϕ are calculated from the EVHRG model. Taking the AdS/CFT lower bound for $\eta/s = 1/(4\pi)$ [5], the value of ϕ at τ_c is found as $\phi_c = \frac{s_c}{3\pi\tau_c}$ with $s_c = s(\tau_c)$. Here τ_c is the time at $T = T_c$.

The authors in Ref. [41] have shown that for a hadronic medium, the equilibration times of kaons and protons are larger as compared to that of pions. Also to be noted is that pions, being the least massive of all hadrons, are abundantly produced at the chemical freeze-out, making them the dominant component of the hadron gas phase. Thus, in the present work, we have approximated the dynamics or evolution of the hadronic phase to be determined by pions [41]. We have considered two different cases in this regard: (a) massless pionic medium and (b) massive pionic medium. The equations of system evolution for the massless case are already available in literature [35, 37] and are given by,

$$\frac{dT}{d\tau} = -\frac{T}{3\tau} + \frac{\phi}{12aT^3\tau} \quad (5)$$

$$\frac{d\phi}{d\tau} = -\sigma b T^3 \phi - \frac{1}{2} \left(\frac{1}{\tau} - 5 \frac{1}{T} \frac{dT}{d\tau} \right) + \frac{8aT^4}{9\tau} \quad (6)$$

where the constants are defined as $a = \pi^2/30$ and $b = 3\zeta(3)/\pi^2$.

The cooling rate equations for the massive medium are derived below.

B. Cooling Law for Massive Pionic Medium

We consider the case of a massive pion gas in the Boltzmann limit. It is a well-known result that the pressure is proportional to the particle number density times the temperature [42];

$$P = a'nT \quad (7)$$

where a' is the proportionality constant ($a' \approx 1$ in the temperature range of our interest). Now, using $P = c_s^2 \varepsilon$, we get,

$$\varepsilon = \frac{a'nT}{c_s^2} \quad (8)$$

On using Eq.7 and Eq.8, the energy equation Eq.1 is modified accordingly,

$$\frac{dT}{d\tau} \left[T \frac{\partial n}{\partial T} + n \right] = -\frac{nT}{\tau} (c_s^2 + 1) + \frac{\phi c_s^2}{a'\tau} \quad (9)$$

here, $\frac{\partial n}{\partial T}$ can be obtained using Eq.29;

$$\frac{\partial n}{\partial T} = \frac{\varepsilon}{T^2} = \frac{a'n}{c_s^2 T} \quad (10)$$

Thus Eq.9 is modified as;

$$\frac{dT}{d\tau} \left[T \frac{a'n}{c_s^2 T} + n \right] = -\frac{nT}{\tau} (c_s^2 + 1) + \frac{\phi c_s^2}{a'\tau} \quad (11)$$

which, on solving, gives the temperature evolution for a massive viscous medium,

$$\frac{dT}{d\tau} = -\frac{c_s^2 T}{\tau} \left(\frac{c_s^2 + 1}{c_s^2 + a'} \right) + \frac{\phi c_s^4}{a'n\tau(c_s^2 + a')} \quad (12)$$

In the case of a massive perfect fluid ($\phi = 0$), this equation reduces to,

$$\frac{dT}{d\tau} = -\frac{c_s^2 T}{\tau} \left(\frac{c_s^2 + 1}{c_s^2 + a'} \right) \quad (13)$$

It is to be noted here that on replacing $a' = 1$, $c_s^2 = 1/3$, and $P = aT^4$, Eq.12 reduces to Eq.5, which is the temperature cooling rate at the massless limit.

The effect of viscosity in Eq.12 is determined by solving Eq.4, which can be solved in the Boltzmann limit by making use of the results obtained in [38, 40]. β_2 is generally defined as,

$$\beta_2 = \frac{1}{2\bar{\eta}^2 P} \left(1 + \frac{6\bar{\eta}}{\beta} \right) \quad (14)$$

where $\beta = m/T$ and $\bar{\eta} = \frac{\varepsilon + P}{nm} = \frac{(c_s^2 + 1)a'T}{m}$ with m being the rest mass of the particle.

$$\beta_2 = \frac{1}{2} \left[\left(\frac{(c_s^2 + 1)a'T}{m} \right)^2 a'nT \right]^{-1} \left[1 + \frac{6(c_s^2 + 1)a'T^2}{m^2} \right] \quad (15)$$

which on solving gives,

$$\beta_2 = \frac{1}{2} \left[\frac{m^2 + 6(c_s^2 + 1)a'T^2}{(c_s^2 + 1)^2 (a'T)^3 n} \right] \quad (16)$$

From Eq.16, the quantity $\frac{\beta_2}{T}$ is now given by,

$$\frac{\beta_2}{T} = \frac{1}{2a'^2 n (c_s^2 + 1)} \left[\frac{m^2}{T^4 (c_s^2 + 1) a'} + \frac{6}{T^2} \right] \quad (17)$$

which may now be used to find,

$$\frac{d}{d\tau} \left(\frac{\beta_2}{T} \right) = \frac{d}{dT} \left(\frac{\beta_2}{T} \right) \frac{dT}{d\tau} \quad (18)$$

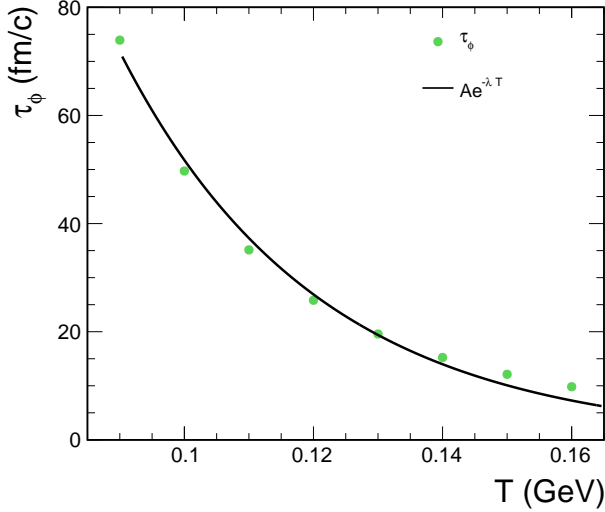


FIG. 1. Relaxation time of a massive pion gas as a function of temperature (T). The fit parameters obtained are $A = 1362.73 \pm 212.198$ fm/c and $\lambda = 32.7087 \pm 1.5375$ GeV $^{-1}$.

$$\frac{d\phi}{d\tau} = -\frac{\phi}{\tau_\phi} - \frac{\phi}{2} \left[\frac{1}{\tau} - \frac{T(c_s^2 + 1)a'^2}{m^2 + 6(c_s^2 + 1)a'T^2} \left\{ \frac{12}{a'} + \frac{6}{c_s^2} + \frac{m^2}{T^2(c_s^2 + 1)a'} \left(\frac{4}{a'} + \frac{1}{c_s^2} \right) \right\} \frac{dT}{d\tau} \right] + \frac{4}{3\tau} \frac{T^3(c_s^2 + 1)^2 a'^3 n}{m^2 + 6(c_s^2 + 1)a'T^2} \quad (22)$$

The only unknown quantity in Eq.22 is the relaxation time (τ_ϕ). The particle-dependent relaxation time for a hadron gas can easily be obtained using the Boltzmann Transport Equation (BTE) as [22, 43];

$$\tilde{\tau}_i^{-1} = \sum_j n_j \langle \sigma_{ij} v_{ij} \rangle \quad (23)$$

Eq.23 is used to find the pion relaxation times at different temperatures and the values obtained are fit by an exponential function ($\tau_\phi = A \exp(-\lambda T)$) as shown in Fig.1 to get an approximate dependence on temperature. This function is further used in Eq.22.

Eq.13 and Eq.22 describe the cooling rate for massive pion gas. In our calculations, we assume $a' = 1$ and $m_\pi = 0.139$ GeV.

C. Transverse Correction to the Cooling Law

The effect of transverse expansion can be included in the 1+1D scaling solution for the partonic state by considering that cooling is defined by the transverse expanded time $\tau_{tr} > \tau$; *i.e.* $T_{tr}(\tau) < T(\tau)$ [7, 8, 44] where τ is the proper time. This would also imply that the temperature cooling begins at a lower temperature $T_{tr}(\tau_0) < T_0(\tau_0)$, τ_0 being the initial thermalization time. Such a consideration makes cooling faster due

required to solve Eq.4. From Eq.17,

$$\frac{d}{dT} \left(\frac{\beta_2}{T} \right) = \frac{1}{2a'^2 n (c_s^2 + 1)} \left[-\frac{4m^2}{T^5 (c_s^2 + 1)a'} - \frac{12}{T^3} \right] + \left[\frac{m^2}{T^4 (c_s^2 + 1)a'} + \frac{6}{T^2} \right] \times \left[-\frac{1}{2a'^2 n^2 (c_s^2 + 1)} \frac{\partial n}{\partial T} \right] \quad (19)$$

On using Eq.10, we get,

$$\frac{d}{dT} \left(\frac{\beta_2}{T} \right) = \frac{1}{2a'^2 n (c_s^2 + 1)} \left[-\frac{4m^2}{T^5 (c_s^2 + 1)a'} - \frac{12}{T^3} \right] + \frac{1}{2a' n c_s^2 (c_s^2 + 1)} \left[-\frac{m^2}{T^5 (c_s^2 + 1)a'} - \frac{6}{T^3} \right] \quad (20)$$

which further reduces to,

$$\frac{d}{dT} \left(\frac{\beta_2}{T} \right) = -\frac{1}{2a' n (c_s^2 + 1) T^3} \left[\frac{12}{a'} + \frac{6}{c_s^2} + \frac{m^2}{T^2 (c_s^2 + 1) a'} \left(\frac{4}{a'} + \frac{1}{c_s^2} \right) \right] \quad (21)$$

Using Eq.16, Eq.18 and Eq.21 in Eq.4 gives,

to the effect of transverse expansion. Thus, due to transverse expansion from the initial phase of collision, the system achieves chemical freeze-out temperature, T_c , earlier than simple 1+1D expansion.

Let us define chemical freeze-out time as τ_{QGP} . In the case of ideal expansion without transverse cooling, one may roughly assume that the QGP fireball lifetime $\tau_{QGP}^{id} = R_T$ [45]. Here R_T is the transverse radius obtained from MC Glauber model [46]. Taking a similar approach but with the transverse expansion, we may assume hadronization to take place when $\tau_{tr} = R_T$. Now defining $\tau_{tr} \cong \tau_{QGP}^{tr} + \frac{R_T}{c_s} \frac{\sqrt{2}-1}{\sqrt{2}}$, τ_{QGP}^{tr} may be easily determined [44]. τ_{QGP}^{tr} is further used as the hadronization time τ_c defined earlier as the initial condition to obtain the hydrodynamical evolution of the hadronic phase.

The left panel of Fig.2 compares the temperature evolution of first-order (FO) and second-order (SO) hydrodynamic models along with the case for a perfect fluid (PF) considering massless pions. It is clear that viscous terms make cooling slower. The second-order theory shows a much faster cooling rate than the first-order theory. The effect of particle mass makes cooling slower, as observed in the perfect fluid limit. The right panel of Fig.2 shows the impact of particle mass on the viscous component, which slows down cooling by generating

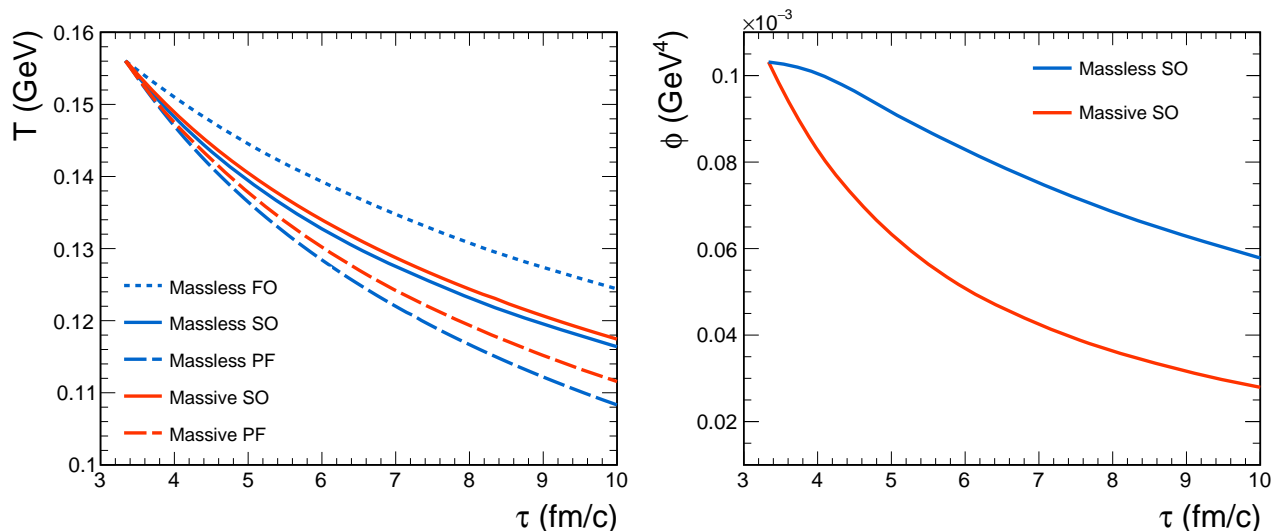


FIG. 2. (Color Online) (Left) Temperature evolution as a function of time for both massive and massless constituent pions. The initial temperature is taken as $T_c = 0.156$ GeV to start the cooling law from the chemical freeze-out [33, 34]. (Right) Comparison of the viscous component as a function of time for massive and massless second-order hydrodynamics.

more heat. In the case of massless particles, viscosity is higher and decays slowly as compared to the massive case. Thus, slowing down of the cooling for massive cases is opposed by the lower viscosity in second-order hydrodynamics as compared to the massless case. An interplay of these effects can be seen in the massive second-order results in the left panel, which is very close to the massless condition albeit slightly slower. In the following, we consider only the second order cooling scenario as the first order solution is acausal and leads to unstable solutions [35].

The validity of hydrodynamics is governed by the Knudsen number (Kn). Knudsen number describes the probability of collisions between the particles in the system. Knudsen number, $Kn \ll 1$, demonstrates that system size is larger than the mean free path, indicating thermalization. Therefore, it becomes feasible to study the medium evolution under hydrodynamics. Knudsen number is given by,

$$Kn = \lambda/D \quad (24)$$

where, $\lambda = \frac{1}{\sqrt{2}n\sigma}$ is the mean free path of the system and $D = 2R$ is the characteristic system size. R denotes the transverse radius of the system. n and $\sigma = 4\pi r_h^2$ are the number density and the interaction cross section within the particles of the medium, respectively. Hydrodynamic evolution ends and equilibrium breaks down at the moment when the mean free path becomes greater than the system size, *i.e.* at $Kn > 1$ [21]. The time-dependent transverse radius used in Eq.24 can be obtained following the method given in [44] where the effective radius at a time $\tau > \tau_i$ is given by,

$$R \cong R_i \left[1 + \frac{1}{6} \sqrt{\frac{1}{\tau_i}} \frac{(\tau - \tau_i)^{3/2}}{R_i} \right] \quad (25)$$

where τ_i is the proper time at the previous instant.

III. HADRONIZATION AND TRANSPORT

At the end of the QGP phase, the deconfined quarks and gluons transition into hadrons, entering the hadronic phase. As a result of confinement, physical observables like particle spectra, flow, fluctuations and correlations, etc. in QCD are required to be defined in terms of hadrons. The dynamics of interactions within the hadronic phase can affect these observables. These interactions involve both elastic scatterings, which change the momentum distribution without altering the particle composition, and inelastic processes, such as resonance formation and decay, that modify the chemical composition of the hadronic matter. This transport and evolution of hadrons in the hadronic phase strongly influence the final particle yields. In this section, we explore the initial hadronization at chemical freeze-out, which is further followed by the influence of interactions during the evolution on resonance particle yields.

A. Statistical Hadronization

The hadronization of the QCD matter is crucial to exploring QCD thermodynamics, and this transformation is effectively captured through the use of statistical thermal

models, such as the Ideal Hadron Resonance Gas (HRG) model. Within the HRG model, the partition function for the i^{th} hadron in the Grand Canonical Ensemble is given by [47];

$$\ln Z_i^{\text{id}} = \pm \frac{V g_i}{2\pi^2} \int_0^\infty p^2 dp \ln \{1 \pm \exp[-(E_i - \mu_i)/T]\} \quad (26)$$

Knowing the partition function, one can calculate the pressure P_i , energy density ε_i , number density n_i , and entropy density s_i as given,

$$P_i^{\text{id}}(T, \mu_i) = \pm \frac{T g_i}{2\pi^2} \int_0^\infty p^2 dp \ln \{1 \pm \exp[-(E_i - \mu_i)/T]\} \quad (27)$$

$$\varepsilon_i^{\text{id}}(T, \mu_i) = \frac{g_i}{2\pi^2} \int_0^\infty \frac{E_i p^2 dp}{\exp[(E_i - \mu_i)/T] \pm 1} \quad (28)$$

$$n_i^{\text{id}}(T, \mu_i) = \frac{g_i}{2\pi^2} \int_0^\infty \frac{p^2 dp}{\exp[(E_i - \mu_i)/T] \pm 1} \quad (29)$$

$$s_i^{\text{id}}(T, \mu_i) = \pm \frac{g_i}{2\pi^2} \int_0^\infty p^2 dp \left[\ln \{1 \pm \exp[-(E_i - \mu_i)/T]\} \pm \frac{(E_i - \mu_i)/T}{\exp[(E_i - \mu_i)/T] \pm 1} \right] \quad (30)$$

In the above equations g_i , $E_i = \sqrt{p^2 + m_i^2}$ and μ_i are the degeneracy, energy and chemical potential of the i^{th} hadron, respectively. μ_i is given by,

$$\mu_i = B_i \mu_B + S_i \mu_S + Q_i \mu_Q \quad (31)$$

where B_i , S_i , and Q_i are the baryon number, strangeness, and electric charge of the i^{th} hadron. Here, μ_B , μ_S , μ_Q are the baryon, strange, and charge chemical potentials, respectively.

Ideal HRG can be further extended by the inclusion of van der Waals (VDW) repulsive interactions between hadrons by considering a fixed volume to be occupied by each hadron (Excluded Volume HRG (EVHRG)). If $v = 16\pi r_h^3/3$ is the volume occupied by each hadron where r_h is the hard-core radius, then the above-mentioned thermodynamic quantities are given by [42, 47],

$$P^{\text{ev}}(T, \mu) = \kappa P^{\text{id}}(T, \mu), \quad (32)$$

$$\varepsilon^{\text{ev}}(T, \mu) = \frac{\kappa \varepsilon^{\text{id}}(T, \mu)}{1 + \kappa v n^{\text{id}}(T, \mu)} \quad (33)$$

$$n^{\text{ev}}(T, \mu) = \frac{\kappa n^{\text{id}}(T, \mu)}{1 + \kappa v n^{\text{id}}(T, \mu)} \quad (34)$$

$$s^{\text{ev}}(T, \mu) = \frac{\kappa s^{\text{id}}(T, \mu)}{1 + \kappa v n^{\text{id}}(T, \mu)} \quad (35)$$

where κ is the excluded volume suppression factor given by,

$$\kappa = \exp\left(\frac{v P^{\text{ev}}}{T}\right) \quad (36)$$

These models have been used extensively to study particle production in nucleus-nucleus collisions. From these studies, it has been observed that particle yields in the final state can be explained with considerable precision by these models at temperatures that are in agreement with the phase transition temperature predicted by LQCD [6, 48, 49]. In the following, we use the EVHRG model to determine the initial yields considering the chemical freeze-out temperature to be equal to $T_c = 156$ MeV as given by the Wuppertal-Budapest collaboration [33, 34].

B. Kinetic Formation Model for Resonance Particles

Several resonance particles are produced in the final state of pp and heavy-ion collisions with lifetimes varying from 1.1 fm/c ($f_2(1270)$) to 46.3 fm/c ($\phi(1020)$). Such a wide range in their lifetimes provides an excellent opportunity to use them as probes to study the system formed in relativistic nuclear collisions [23, 50–53]. In the subsequent calculations, we have used three different resonance particles, namely, $\rho(770)^0$, $K^*(892)^0$, and $\phi(1020)$. Out of these, the $K^*(892)^0$ meson occupies a sweet spot with a lifetime of 4.16 fm/c, making it a good probe to study the hadronic phase and hadronic phase lifetime as performed in Ref.[23]. If the resonance decays within the hadronic phase, then the decay products are subject to interactions before kinetic freeze out, which alters their momentum and prevents their reconstruction (re-scattering) ($\rho(770)^0 \rightarrow \pi^+\pi^-$, $K^*(892)^0 \rightarrow \pi K$, $\phi(1020) \rightarrow K^+K^-$). Similarly, hadrons in the medium can interact together to form resonances that may live up to the kinetic freeze-out allowing a successful reconstruction (regeneration) ($\pi^+\pi^- \rightarrow \rho(770)^0$, $\pi K \rightarrow K^*(892)^0$, $K^+K^- \rightarrow \phi(1020)$). Thus, it is imperative to include both of these effects in the calculations while studying the final resonance yields.

In this respect, we use a modified version of the kinetic formation model used to explain the yield of J/ψ meson in the final state [54, 55]. This model was subsequently modified to include transverse momentum dependence of the decay and regeneration cross-sections [7, 8]. According to this model, the final state yield of resonance particles ($A \rightleftharpoons BC$) is given by,

$$N_f^A(\tau_f, p_T) = \epsilon(\tau_f, p_T) \lambda_D(\tau_f, p_T) [N_i^A(\tau_c, p_T) + N^B(p_T) N^C(p_T) \times \int_{\tau_c}^{\tau_f} \Gamma_F(p_T) [V(\tau) \epsilon(\tau, p_T) \lambda_D(\tau, p_T)]^{-1} d\tau] \quad (37)$$

where $\lambda_D(\tau, p_T)$ and $\epsilon(\tau, p_T)$ give the contribution due to natural decay and co-moving hadrons, respectively, to re-scattering at time τ while $\Gamma_F(p_T)$ gives the effect of regeneration.

The $V(\tau)$ used in Eq.37 is the time-dependent volume of the evolving system. It is obtained considering the isentropic evolution of the hadronic phase. On the hadronic evolution, Andronic and Munzinger et al., based on their study, have implied that any further evolution of the fireball after T_c has to be close to isentropic [6, 56]. Further, in Ref. [45], the authors have quantitatively shown that for viscous hydrodynamic evolution, entropy production is minimal for the extended period when freeze-out is introduced. Thus, the volume profile of the medium $V(\tau, b)$ is obtained as,

$$V(\tau, b) = \frac{V_c(\tau_c, b)s_c(\tau_c)}{s(\tau)} \quad (38)$$

here, $V_c(\tau_c, b) = \tau_{tr}A_T(b)$ is the initial volume at τ_0 . The A_T is the transverse overlap area obtained from the MC Glauber model [46].

Furthermore, the variables $N_i^C(\tau_c, p_T)$, $N^B(p_T)$ and $N^C(p_T)$ used in Eq. 37 are the p_T -dependent numbers of resonance particles and their decay products at chemical freeze-out determined through the EVHRG model. $N^B(p_T)$ and $N^C(p_T)$ are estimated such that their combination can produce a resonance particle at given p_T .

1. Regeneration

Regeneration of resonance particles in the hadronic phase is modeled in Eq.37 through $\Gamma_F(p_T)$, which is given by,

$$\Gamma_F(p_T) = \langle \sigma_{reg}^A(p_T)v_{rel} \rangle_{B,C} \quad (39)$$

Here, $\sigma_{reg}(p_T)$ is the regeneration cross-section, and v_{rel} is the relative velocity between the particles. For $\rho(770)^0$ and $K^*(892)^0$ mesons, the temperature-dependent regeneration cross-sections ($\sigma_{reg}(T)$) are given by [57],

$$\sigma_{reg}^\rho(T) = 54.1 \left(\frac{T/T_c - 0.42}{0.18} \right)^{3.3} \exp \left[3.3 \left(1 - \frac{T/T_c - 0.42}{0.18} \right) \right] + 5.32 \left(\frac{T/T_c - 0.42}{0.5} \right)^{84} \exp \left[84 \left(1 - \frac{T/T_c - 0.42}{0.5} \right) \right] \quad (40)$$

$$\sigma_{reg}^{K^*}(T) = 42.2 \left(\frac{T/T_c - 0.5}{0.115} \right)^{1.83} \exp \left[1.83 \left(1 - \frac{T/T_c - 0.5}{0.115} \right) \right] + 4.95 \left(\frac{T/T_c - 0.5}{0.407} \right)^{50} \exp \left[50 \left(1 - \frac{T/T_c - 0.5}{0.407} \right) \right] \quad (41)$$

where the crossover temperature was taken to be $T_c = 0.175$ GeV. In the absence of such temperature dependent parameterizations for $\phi(1020)$ mesons, we use the

vacuum cross-section of 8.05 mb [58] at all temperatures (*i.e.*, $\sigma_{reg}^\phi(T) = 8.05$ mb).

The temperature experienced by the resonance particle may be different from the medium temperature. Thus, we use the relativistic Doppler shift due to the relative velocity of resonance (v_r) as compared to the medium to obtain the effective temperature felt by the resonance particle. The effective temperature is given by [7, 59, 60]

$$T_{eff}(\tau, p_T) = T(\tau) \frac{\sqrt{1 - |v_r|^2}}{2|v_r|} \ln \left[\frac{1 + |v_r|}{1 - |v_r|} \right] \quad (42)$$

To calculate v_r , we have used the medium velocity $v_m = 0.5 c$ comparable to the expansion velocity obtained from blastwave fits to data [61] and resonance velocity $v_A = p_T/E_T$. The transverse energy E_T is given by $E_T = \sqrt{p_T^2 + m_A^2}$. Thus, the p_T -dependent regeneration cross-sections ($\sigma_{reg}^A(p_T)$) are obtained from the temperature dependent cross-sections ($\sigma_{reg}^A(T)$) by using $T_{eff}(\tau, p_T)$ in place of T .

2. Decay

The re-scattering effect introduced in Eq.37 has been modeled to include two different effects. Resonance particles produced at chemical freeze-out can undergo natural decay ($A \rightarrow BC$). They might also decay as a result of interaction with another particle within the medium (co-moving hadron) ($AX \rightarrow BCX$). We consider that the resonance particle is re-scattered in both cases. The contribution due to natural decay is given by,

$$\lambda_D(\tau, p_T) = \exp \left(- \frac{\tau - \tau_c}{\tau_l(p_T)} \right) \quad (43)$$

$\tau_l(p_T) = \tau_{reso}\gamma(p_T)$ is the lifetime of the resonance particle (τ_{reso}) multiplied by the Lorentz factor. In our calculations, we have considered the Lorentz factor to be $\gamma(p_T) = \sqrt{1 + (p_T/mc)^2}$ [23]. The effect of co-moving hadrons is modeled based on the kinetic model [54, 55],

$$\epsilon(\tau, p_T) = \exp \left[- \int_{\tau_c}^{\tau} \Gamma_D(p_T) N_{co}[V(\tau)]^{-1} d\tau \right] \quad (44)$$

where $\Gamma_D(p_T)$ is the decay rate of resonances, with transverse momentum p_T , averaged over the co-moving hadron momentum distribution and is given by

$$\Gamma_D(p_T) = \langle \sigma_{co}^A(p_T)v_{rel} \rangle_{A,co} \quad (45)$$

Here, $\sigma_{co}^A(p_T)$ is the p_T -dependent decay cross-section. This decay cross-section is obtained by using detailed balance from the regeneration cross-section ($\sigma_{reg}^A(p_T)$) [7, 55].

The thermal averaged cross-section times relative velocity used in Eq.39 and Eq.45 is given by [22, 43];

$$\langle \sigma_{ij} v_{ij} \rangle = \frac{\sigma \int p_i p_j E_i dE_i E_j dE_j d\cos\theta f_i^0 f_j^0 \times \sqrt{\frac{(E_i E_j - p_i p_j \cos\theta)^2 - (m_i m_j)^2}{E_i E_j - p_i p_j \cos\theta}}}{\int p_i p_j E_i dE_i E_j dE_j d\cos\theta f_i^0 f_j^0} \quad (46)$$

E_i and E_j are particle energies and are integrated in the limit m_i to ∞ and m_j to ∞ , respectively. The limit of integration of $\cos\theta$ runs from -1 to +1. f_i^0 is the particle distribution function, which is given by,

$$f_i^0 = \exp\left(-\frac{E_i - \mu}{T}\right) \quad (47)$$

where E_i is the energy of i^{th} particle, μ is the baryochemical potential, which is approximated to be zero in our calculations, and T is the temperature.

IV. RESULTS AND DISCUSSION

The hadronic medium considered in this work consists of all hadrons and resonances with masses up to 2.25 GeV given in the particle data book [62]. Since the properties of the medium depend on the parameter r_h , it has to be chosen appropriately. The repulsive interactions being mediated by ω meson and the range of interaction being inversely proportional to the mass of the mediator, we have chosen the hard-core radius, $r_h = 0.25$ fm to incorporate repulsive interactions. This radius is chosen to be uniform for all hadrons.

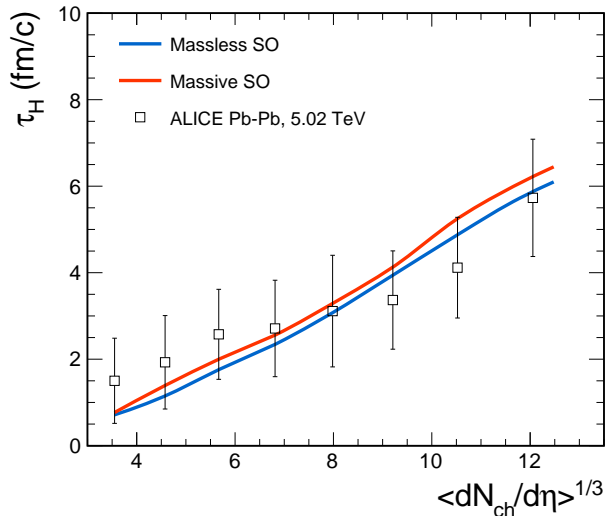


FIG. 3. (Color Online) Hadronic phase lifetime obtained from our calculations and are compared with the results obtained for Pb-Pb $\sqrt{s_{NN}} = 5.02$ TeV collisions at ALICE [23].

Knudsen number is an important parameter as it indicates the applicability of hydrodynamics in the medium. As discussed in Sec.II, we have used this parameter to

obtain the endpoint for hydrodynamics (τ_f). Finding τ_f allows us to estimate the hadronic phase lifetime (τ_H) simply by calculating the difference between the initial (τ_c) and final time (τ_f). In Fig.3, we depict this hadronic phase lifetime obtained in our calculations for both massive and massless second-order hydrodynamics and compared it with the results obtained in 5.02 TeV Pb-Pb collisions at LHC [23]. The massive second-order theory, being slightly slower than the massless case (as seen in Fig.2), gives a higher lifetime. A reasonable agreement is observed between our calculations and the experimental results in both cases.

Further, we investigated the p_T -dependent natural decay, co-moving hadron-induced decay, and regeneration of the resonance particles within the hadronic phase as given by Eq. 43, 45, and 39, respectively. The results for the (0-5)% centrality Pb-Pb collisions at $\sqrt{s_{NN}} = 5.02$ TeV with these parameters are presented in Fig.4. In the left panel of Fig.4, the natural decay rate is analyzed as a function of momentum for different resonance particles. At high p_T , time dilation causes λ_D to increase and approach unity. The impact of particle lifetime on the survival probability is evident, as the $\phi(1020)$ meson with $\tau_{reso} = 46.3$ fm/c is relatively unaffected beyond $p_T = 2$ GeV/c. In contrast, the yields of $\rho(770)^0$ mesons, which have $\tau_{reso} = 1.3$ fm/c, are reduced over an extended p_T range. The middle and right panels of Fig.4 display the p_T -dependent interaction rates for co-mover-induced decay and regeneration, respectively. It is observed that decay and regeneration are more likely at low p_T for all the considered resonances. These probabilities decrease further and saturate towards high p_T , which can be attributed to the initial particle production at these p_T intervals. It is more probable for particles at low p_T to move together, favoring the interaction, compared to particles with high p_T . In the following discussions, “ND”, “CMD”, and “R” represent natural decay, co-moving hadrons-induced decay, and regeneration effects, respectively. The individual effects of the regeneration, decay due to co-moving hadrons, and natural decay are explicitly studied.

The combined effects of these mechanisms on the resonance yields are further studied and shown in Fig.5 as a function of p_T . The particle ratios are shown only for the “ND+CMD+R” and “ND+CMD” cases, as the “ND+R” case is nearly identical to the “ND+CMD+R” scenario. In all the three particle ratios considered, a qualitative agreement is obtained for $p_T < 3$ GeV for the “ND+CMD+R” case beyond which the particle ratios are overestimated. However, a complete description of

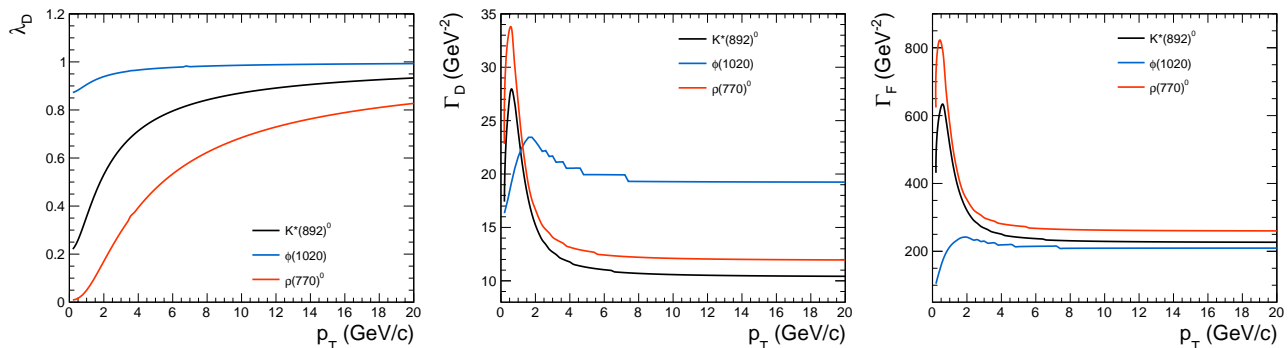


FIG. 4. (Color Online) The natural decay parameter λ_D (left), dissociation reactivity Γ_D (center) and regeneration reactivity Γ_F (right) explored as a function of transverse momentum (p_T) for $K^*(892)^0$, $\phi(1020)$ and $\rho(775)^0$.

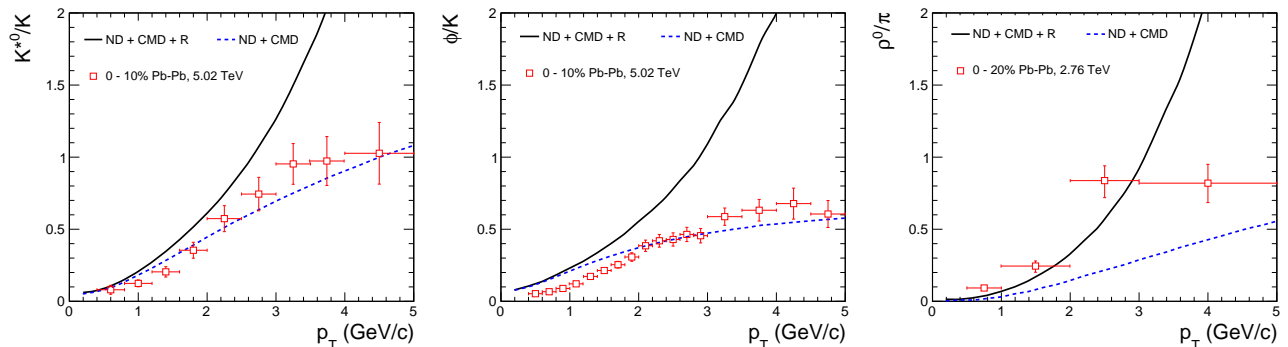


FIG. 5. (Color Online) Transverse momentum (p_T) dependent $K^*(892)^0/K$ (left), $\phi(1020)/K$ (center) and $\rho(775)^0/\pi$ (right) ratios are compared with the results from the ALICE data [23, 64].

the full p_T range is not expected due to the limitations of hydrodynamic calculations and its ability to account for high p_T particles. In the absence of regeneration effects, these ratios tend to be much lower towards higher p_T . This indicates that our model overestimates regeneration effects towards the high p_T region. Such an overestimation is mainly due to the effect of the initially obtained p_T -dependent daughter particle numbers, which was seen to overshadow the initial resonance particle production. Thus, the final particle numbers obtained at high p_T tend to increase rapidly. A more complete description would be needed to account for these effects and obtain the saturating out of particle ratios to high p_T seen experimentally.

Fig.6 depicts the final state particle ratios of resonances to stable particles obtained in heavy ion collisions. The left, middle, and right panels of Fig.6 compare the values obtained in our calculations for massive second-order theory to the experimentally obtained $K^*(892)^0/K$, $\phi(1020)/K$ and $\rho(775)^0/\pi$ ratios [23, 63–66]. The massless second-order case is not shown here as it does not account for the relatively realistic scenario. Also, there is a small change in hadronic phase lifetime as compared to the massive case (shown in Fig. 3). A con-

siderable agreement with experimental values is obtained for $K^*(892)^0/K$ and $\phi(1020)/K$ estimates, even though $\sigma_{reg}^\phi(T)$ is approximated to be constant. At the same time, $\rho(775)^0/\pi$ values are underestimated, especially at the high multiplicity regions. The natural decay component plays an important part in determining the trends obtained for $K^*(892)^0/K$ and $\rho(775)^0/\pi$ estimates due to their sufficiently small lifetimes. For $\phi(1020)/K$, λ_D being large as seen in Fig.4, there is very little change due to natural decay. It can also be seen that both co-moving hadrons-induced decay and regeneration effects play important roles at high multiplicity bins, while their impact on low multiplicities is marginal. Our study suggests that these effects must be considered while using resonances as a probe to study the hadronic phase produced in relativistic nuclear collisions.

V. SUMMARY

In this study, a hydrodynamic description is employed in the hadronic phase motivated through the dimensionless parameter, Knudsen number (Kn), which implies the applicability of hydrodynamics. We have found that the lifetime obtained through a hydrodynamic

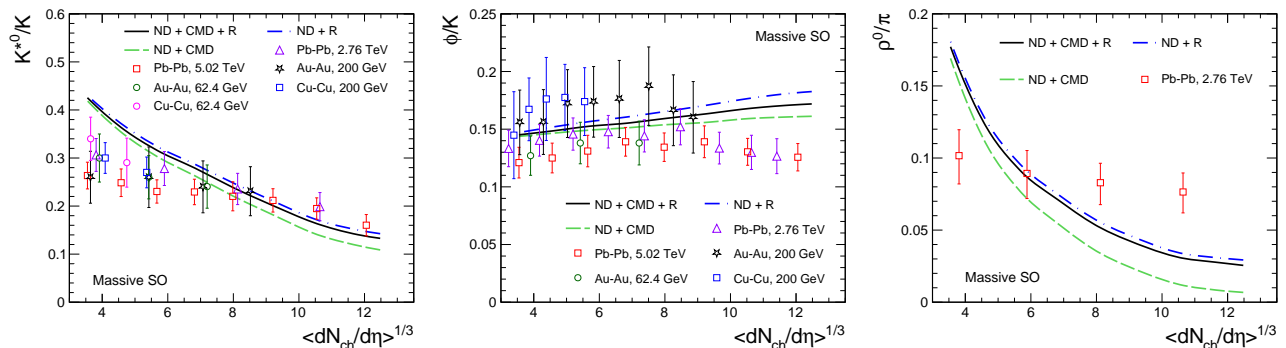


FIG. 6. (Color Online) The estimated ratios of $K^*(892)^0/K$ (left), $\phi(1020)/K$ (center) and $\rho(775)^0/\pi$ (right) obtained using our model and compared with the results from ALICE and RHIC with different colliding species [23, 63–66].

description of the hadronic phase is in close agreement with the results obtained at the ALICE experiment at LHC. Further, it is observed that the hadronic phase lifetime increases with the system size, which is manifested here in terms of charged particle multiplicity ($\langle dN_{ch}/d\eta \rangle$). We have shown that in heavy-ion collisions, the hadronic phase lifetime varies between 0.5 fm to ~ 6 fm from ultra-peripheral to most-central collisions, respectively. We have also explored the yield modification of the resonance particles due to the natural decay and dissociation due to the co-moving hadrons during the hydrodynamic evolution of the hadronic phase. The regeneration of the resonances due to the combination of the required hadrons is also studied, and it is found that regeneration plays a crucial role besides dissociation mechanisms in obtaining the net yield of the resonance particles moving in the expanding system. The obtained results are compared with corresponding experimental data. These results qualitatively explain the experimental results at low $p_T \leq 3$ GeV as expected because at high p_T , the applicability of the hydrodynamics is questionable. Further, p_T -integrated resonance particle ratios are obtained against charged particle multiplicity and compared with correspond-

ing experimental results showing considerable agreement.

The present study explored the applicability of hydrodynamics, considering only massive pions as a component of the thermalized fluid using 1+1D viscous Bjorken-like flow. However, other abundant hadrons must be included as a part of the fluid along with an extended 3+1D viscous hydrodynamics for a comprehensive study. Furthermore, our estimates could have uncertainties due to the interaction cross-sections chosen from EVHRG, as the interaction cross-sections are poorly known near the chemical freeze-out boundary. These can be addressed by a proper estimation of the hadronic interaction cross-sections.

ACKNOWLEDGEMENT

Ronald Scaria acknowledges CSIR, the Government of India, for the research fellowship. Raghunath Sahoo and Captain R. Singh acknowledge the financial support under DAE-BRNS, the Government of India, Project No. 58/14/29/2019-BRNS. The authors acknowledge the Tier-3 computing facility in the experimental high-energy physics laboratory of IIT Indore, supported by the ALICE project.

-
- [1] I. Arsene et al. (BRAHMS Collaboration), Nucl. Phys. A **757**, 1 (2005).
 - [2] B. B. Back et al. (PHOBOS Collaboration), Nucl. Phys. A **757**, 28 (2005).
 - [3] J. Adams et al. (STAR Collaboration), Nucl. Phys. A **757**, 102 (2005).
 - [4] K. Adcox et al. (PHENIX Collaboration), Nucl. Phys. A **757**, 184 (2005).
 - [5] P. Kovtun, D.T. Son and A.O. Starinets, Phys. Rev. Lett. **94**, 111601 (2005).
 - [6] A. Andronic, P. Braun-Munzinger, K. Redlich and J. Stachel, Nature **561**, 321 (2018).
 - [7] C. R. Singh, S. Ganesh, and M. Mishra, Eur. Phys. J. C **79**, 147 (2019).
 - [8] C. R. Singh, S. Deb, R. Sahoo, and J. Alam Eur. Phys. J. C **82**, 542 (2022).
 - [9] H. Bebie, P. Gerber, J. L. Goity, and H. Leutwyler, Nucl. Phys. B **378**, 95 (1992).
 - [10] A. Motornenko, V. Vovchenko, C. Greiner and H. Stoecker, Phys. Rev. C **102**, 024909 (2020).
 - [11] H. Petersen, J. Steinheimer, G. Burau, M. Bleicher and H. Stöcker, Phys. Rev. C **78**, 044901 (2008).
 - [12] Z. W. Lin, C. M. Ko, B. A. Li, B. Zhang and S. Pal, Phys. Rev. C **72**, 064901 (2005).
 - [13] J. Steinheimer, J. Aichelin, M. Bleicher and H. Stöcker, Phys. Rev. C **95**, 064902 (2017).
 - [14] A. G. Knospe, C. Markert, K. Werner, J. Steinheimer, M. Bleicher, Phys. Rev. C **93**, 014911 (2016).

- [15] H. Song, S. A. Bass and U. Heinz, Phys. Rev. C **83**, 024912 (2011).
- [16] N. Demir and S. A. Bass, Phys. Rev. Lett. **102**, 172302 (2009).
- [17] P. Romatschke, Eur. Phys. J. C **75**, 429 (2015).
- [18] J. Berges, S. Borsanyi and C. Wetterich, Phys. Rev. Lett. **93**, 142002 (2004).
- [19] P. Romatschke, Phys. Rev. Lett. **120**, 012301 (2018).
- [20] P. Romatschke and U. Romatschke, Cambridge University Press (2019).
- [21] K. Gallmeister, H. Niemi, C. Greiner and D. H. Rischke, Phys. Rev. C **98**, 024912 (2018).
- [22] R. Scaria, D. Sahu, C. R. Singh, R. Sahoo and J. e. Alam, Eur. Phys. J. A **59**, 140 (2023).
- [23] S. Acharya *et al.* (ALICE Collaboration), Phys. Lett. B **802**, 135225 (2020).
- [24] S. Singha, B. Mohanty, and Z.-W. Lin, Int. J. Mod. Phys. E **24**, 1550041 (2015).
- [25] A. Andronic, P. Braun-Munzinger, and J. Stachel, Phys. Lett. B **673**, 142 (2009).
- [26] J. Cleymans and K. Redlich, Phys. Rev. C **60**, 054908 (1999).
- [27] S. Chatterjee, S. Das, L. Kumar, D. Mishra, B. Mohanty, R. Sahoo, N. Sharma, Adv. High Energy Phys. **2015** 349013 (2015).
- [28] S. Cho and S. H. Lee, Phys. Rev. C **97**, 034908 (2018).
- [29] D. Sahu, S. Tripathy, G. S. Pradhan and R. Sahoo, Phys. Rev. C **101**, 014902 (2020).
- [30] F. Karsch, Lect. Notes Phys. **583**, 209 (2002).
- [31] Y. Aoki, G. Endrodi, Z. Fodor, S. Katz, and K. Szabo, Nature **443**, 675 (2006).
- [32] A. Bazavov *et al.* [HotQCD], Phys. Rev. D **90**, 094503 (2014).
- [33] S. Borsanyi, Z. Fodor, C. Hoelbling, S. D. Katz, S. Krieg, C. Ratti, and K. K. Szabo, JHEP **09**, 073 (2010).
- [34] S. Borsanyi, Z. Fodor, C. Hoelbling, S. D. Katz, S. Krieg and K. K. Szabo, Phys. Lett. B **730**, 99 (2014).
- [35] A. Muronga, Phys. Rev. C **69**, 034903 (2004).
- [36] H. Kouno, M. Maruyama, F. Takagi and K. Saito, Phys. Rev. D **41**, 2903 (1990).
- [37] A. Muronga, Phys. Rev. Lett. **88**, 062302 (2002).
- [38] W. Israel, Ann. Phys. (N.Y.) **100**, 310 (1976).
- [39] J. M. Stewart, Proc. R. Soc. London A **357**, 59 (1977).
- [40] W. Israel and J. M. Stewart, Ann. Phys. (N.Y.) **118**, 341 (1979).
- [41] M. Prakash, M. Prakash, R. Venugopalan and G. Welke, Phys. Rept. **227**, 321 (1993).
- [42] V. Vovchenko, D. V. Anchishkin, and M. I. Gorenstein, Phys. Rev. C **91**, 024905 (2015).
- [43] S. K. Tiwari, S. Tripathy, R. Sahoo and N. Kakati, Eur. Phys. J. C **78**, 938 (2018).
- [44] I. P. Lokhtin and A. M. Snigirev, Phys. Lett. B **378**, 247 (1996).
- [45] P. Hanus, A. Mazeliauskas and K. Reygers, Phys. Rev. C **100**, 064903 (2019).
- [46] C. Loizides, J. Kamin and D. d'Enterria, Phys. Rev. C **97**, 054910 (2018).
- [47] A. Andronic, P. Braun-Munzinger, J. Stachel, and M. Winn, Phys. Lett. B **718**, 80 (2012).
- [48] A. Andronic, P. Braun-Munzinger and J. Stachel, Nucl. Phys. A **772**, 167 (2006).
- [49] J. Stachel, A. Andronic, P. Braun-Munzinger and K. Redlich, J. Phys. Conf. Ser. **509**, 012019 (2014).
- [50] M. Bleicher and J. Aichelin, Phys. Lett. B **530**, 81 (2002).
- [51] G. Torrieri and J. Rafelski, Phys. Lett. B **509**, 239 (2001).
- [52] S. C. Johnson, B. V. Jacak and A. Drees, Eur. Phys. J. C **18**, 645 (2001).
- [53] A. Ilner, J. Blair, D. Cabrera, C. Markert and E. Bratkovskaya, Phys. Rev. C **99**, 024914 (2019).
- [54] R. L. Thews, Nucl. Phys. A **702**, 341 (2002).
- [55] R. L. Thews, M. Schroedter and J. Rafelski, Phys. Rev. C **63**, 054905 (2001).
- [56] A. Andronic, P. Braun-Munzinger, J. Stachel and H. Stocker, Phys. Lett. B **697**, 203 (2011).
- [57] K. Yang, X. M. Xu and H. J. Weber, Phys. Rev. D **96**, 114025 (2017).
- [58] W. X. Li, X. M. Xu and H. J. Weber, Eur. Phys. J. C **81**, 225 (2021).
- [59] F. Nendzig and G. Wolschin, J. Phys. G **41**, 095003 (2014).
- [60] J. Hoelck, F. Nendzig and G. Wolschin, Phys. Rev. C **95**, 024905 (2017).
- [61] S. Acharya *et al.* [ALICE], Phys. Rev. C **101**, 044907 (2020).
- [62] P.A. Zyla *et al.* (Particle Data Group), PTEP **2020**, 083C01 (2020).
- [63] M. M. Aggarwal *et al.* [STAR], Phys. Rev. C **84**, 034909 (2011).
- [64] S. Acharya *et al.* [ALICE], Phys. Rev. C **99**, 064901 (2019).
- [65] B. I. Abelev *et al.* [STAR], Phys. Rev. C **79**, 064903 (2009).
- [66] B. B. Abelev *et al.* [ALICE], Phys. Rev. C **91**, 024609 (2015).